DENOISING AND SEGMENTATION OF MR IMAGES BY COUPLED DIFFUSIVE FILTERS.

FABIANA ZAMA

Abstract. The image denoising and segmentation is a fundamental task in many medical applications based on magnetic resonance image processing. This problem can be solved by means of nonlinear diffusive filters requiring the solution of evolutive partial differential equations. In this work a coupled system of linear and nonlinear diffusion-reaction equations is proposed and tested for denoising and segmentation of magnetic resonance images. The discretization of the coupled system by means of the Finite Element method is reported. The effectiveness of the model has been tested on MR images affected by gaussian, impulsive noise and also in the case of dynamic magnetic resonance images where the data are affected by noise in the frequency domain.

Magnetic Resonance Imaging, Nonlinear Diffusive Filtering, Segmentation, Total Variation, Coupled Pde

1. Introduction

Segmentation of brain tissues in Magnetic Resonance (MR) images plays an indispensable role in medical research and clinical applications such as pathology, radiotherapy treatment and planning, simulations and diagnosis. It is the prerequisite for three dimensional volume visualization, quantitative morphometric analysis and partial volume correction. In dynamic functional brain studies a temporal series of MR images of the same slice of the imaged structure is acquired. Unfortunately the technology and physiological limits on the MR technique make difficult to have simultaneously high temporal and spatial resolution. The reduced-encoding method speeds-up the acquisition time by acquiring a time series of reduced dynamic data sets and one high resolution reference data, collected before the dynamic process. The dynamic data set consists of a small and central part (k-hole) of the k-space (a frequency 2D domain) constituted by the low frequencies along the phase encoded direction. The reference data set provides the a-priori information concerning the high frequencies uncollected during the dynamic process. The k-hole method [2] consist in reconstructing the dynamic images by a 2D inverse Fourier Transform of

the low resolution dynamic data completed with the high frequencies obtained by the reference image. This method is extremely fast but suffers from ringing and Gibbs artifacts that can be compensated by more sophisticated reconstruction methods, such as generalized-series reconstruction methods (RIGR) [2] or by using a posteriori enhancement methods such as the Total Variation (TV) regularization method [4, 3, 18]. TV regularization is a popular approach used in image processing for reducing noise while preserving the edges [1, 5]. In the present work the TV functional is used to define an anisotropic filter to perform image denoising and segmentation at the same time.

Image denoising and segmentation can be formulated using variational principles which in turn require the solution of partial differential equations. In [6] Perona and Malik proposed an anisotropic diffusion scheme for image smoothing. The basic idea of this scheme was to smooth the image while preserving the edges. This was done by using the diffusion equation $u_t = \nabla \cdot (g(\nabla u)\nabla u)$ where u is the image to be smoothed and u_t represents the evolution over time. The function $g(\cdot)$ represents a decreasing diffusivity function. Segmentation is obtained by finding the edges in the smoothed image. The ill-posedness of the Perona Malik scheme has been overcome by several modifications proposed in [7], [9], [8]. Since then numerous models of linear and nonlinear diffusion schemes have been proposed in the literature, a survey of nonlinear methods can be found in [12]. The linear models, involving the standard heat equation, blur image features such as edges displacing them when moving from fine to coarser scales. Nonlinear anisotropic diffusion has been proposed by many researchers, [7], [9], [10]. All these models differ in the diffusivity function. Some of them are also supplemented by a reactive term. Following [13] we present system of two PDEs where a nonlinear diffusion-reaction equation is coupled with a linear diffusion-reaction equation used for enhancing the edge detection process. The solution is computed by means of the Finite Element method (FEM) using the Comsol Multiphysics (CM) primitives integrated with the Matlab functions of the Image Processing Toolbox (IPT) for image image acquisition and display. The numerical implementation of the FEM solution of the proposed coupled is a great programming task. By using the CM primitives it is possible to implement quite easily a matlab based application that allows us to evaluate the results obtained with different parameter values and noise models given by the IPT `imnoise` function. The effectiveness of the model has been tested on MR images affected by gaussian, impulsive noise and also in the case of functional magnetic resonance images affected by noise in the frequency domain.

In section 2 the diffusion reaction model is introduced. The FEM discretization is reported in section 3. Finally in section 4 the results obtained with test problems and different noise models are reported. The conclusions are reported in section 5.

2. The Nonlinear Diffusion Model

The denoising and segmentation filter used in this work is originated by the following nonlinear diffusion reaction equation [13]:

$$\frac{\partial u}{\partial t} = |\nabla u| \nabla \cdot \left(g\left(|\nabla u_\sigma|^2\right) \frac{\nabla u}{|\nabla u|} \right) + \beta |\nabla u| \left(u - u_0\right), \tag{1}$$

with boundary conditions:

$$\mathbf{n} \cdot \left(g\left(|\nabla u_\sigma|^2\right) \frac{\nabla u}{|\nabla u|} \right) = 0$$

where $\mathbf{n}$ is the outward unit vector on the domain boundary and ∇u denotes the gradient of u. The initial condition are:

$$u(x, y, 0) = u_0(x, y)$$

where u_0 is the noisy image to be enhanced. The diffusivity function g has the purpose of selecting locations in the image for smoothing. Using the TV diffusivity function we have:

$$g(s) = \frac{1}{1 + s^2/K}$$

with $K > 0$. Here K plays the role of threshold for distinguishing different regions of the image: points with $s^2 > K$ are regarded as edges, where the diffusivity is small, whereas points with $s^2 < K$ are considered to belong to the interior of a region where the diffusivity is close to 1. The parameter σ is introduced as a smoothing parameter with the purpose of better definition of the edges in the gradient image. Usually u_σ is computed by means of a convolution with a gaussian low pass filter of prescribed standard deviation σ. As observed in [11, 14] u_σ can be computed by means of one diffusion step with constant diffusivity ($g = 1$), i.e. solving the diffusion equation:

$$\frac{\partial u_\sigma}{\partial t} = \nabla \cdot (\nabla u)$$

at time step $t = \sqrt{2\sigma}$. This shows that σ is actually proportional to the time (scale parameter) of the diffusion process. Using this consideration

we derive the following coupled model:

$$\begin{aligned} \frac{\partial w}{\partial t} &= \nabla \cdot (k \nabla w) + \gamma(u - w), \\ \frac{\partial u}{\partial t} &= |\nabla u| \nabla \cdot \left(g\left(|\nabla w|^2\right) \frac{\nabla u}{|\nabla u|} \right) + \beta |\nabla u| \left(u_0 - u\right) \end{aligned} \tag{2}$$

and the following boundary and initial conditions:

$$\begin{aligned} \mathbf{n} \cdot \left(g\left(|\nabla w|^2\right) \frac{\nabla u}{|\nabla u|} \right) &= 0, \\ \mathbf{n} \cdot (k \nabla w) &= 0, \\ u(x, y, 0) &= u_0(x, y) \\ w(x, y, 0) &= u(x, y, 0) \end{aligned}$$

where k is the diffusivity coefficient used to control the gaussian smoothing over integration time and a reaction coefficient γ is introduced in the diffusion model to control distance of the solution w with respect to u.

3. Finite element discretization

Finite Element Methods (FEM) are widely used to discretize and implement the diffusion based models. In this section we describe FEM to solve our coupled model (2).

Let $u(t, x, y)$ be the intensity value of the 2D image defined on the domain $\Omega \equiv [0, n_x] \times [0, n_y]$, $(n_x, n_y \in \mathbb{N})$, and the time domain $J = [0, T]$ such that $(t \in J)$. Let $\mathcal{T}_h$ be a member of quasi uniform triangulations of Ω with

$$\max_{\tau \in \mathcal{T}_h} \operatorname{diam}(\tau) \leq h$$

where $\operatorname{diam}(\tau)$ is the maximum distance among the vertices of the triangle τ. Let us define S_h as the finite dimensional space of continuous function on Ω that reduce to linear functions in each of the triangles of $\mathcal{T}_h$, we pose the semi discrete problem to find $u, w : J \longrightarrow S_h$ such that:

$$\begin{aligned} (w_t, \nu) + (k \nabla w, \nabla \nu) &= \gamma(u - w, \nu), \\ \left(\frac{u_t}{|\nabla u|_\varepsilon}, \nu \right) + \left(\frac{g(|\nabla w|^2)}{|\nabla u|_\varepsilon} \nabla u, \nabla \nu \right) &= \beta \left(u_0 - u, \nu\right), \\ \forall \nu \in S_h \quad t \in J, & \end{aligned} \tag{3}$$

where $(\cdot, \cdot)$ denotes the inner product in $L^2(\Omega)$ and $|\nabla u|_\varepsilon = \sqrt{|\nabla u| + \varepsilon}$ is used to avoid the problem of possible zero gradients. Representing

the solution as

$$u(t,x,y) = \sum_{j=1}^{N_h} u_j(t)\Phi_j(x,y), \quad w(t,x,y) = \sum_{j=1}^{N_h} w_j(t)\Phi_j(x,y)$$

where $\{\Phi_j(x,y)\}_{j=1}^{N_h}$ are the standard basis pyramidal functions, problem (3) can be written as a system of nonlinear ordinary differential equations [17]:

$$\begin{aligned}
\sum_{j=1}^{N_h} w_j'(t)\,(\Phi_j,\Phi_k) + \sum_{j=1}^{N_h} w_j(t)\,(k\nabla\Phi_j,\nabla\Phi_k) = \\
= \gamma \sum_{j=1}^{N_h} (u_j(t) - w_j(t))\,(\Phi_j,\Phi_k) \\
\sum_{j=1}^{N_h} u_j'(t)\left(\frac{\Phi_j}{|\nabla u|_\varepsilon},\Phi_k\right) + \sum_{j=1}^{N_h} u_j(t)\left(\frac{g(|\nabla w|^2)}{|\nabla u|_\varepsilon}\nabla\Phi_j,\nabla\Phi_k\right) = \\
= \beta \sum_{j=1}^{N_h} (\alpha_j - u_j(t))\,(\Phi_j,\Phi_k)\,, \quad k = 1,2,\ldots,N_h \qquad (4)
\end{aligned}$$

Setting $\underline{u} = (u_1(t), u_2(t), \ldots, u_{N_h}(t))$ and $\underline{w} = (w_1(t), w_2(t), \ldots, w_{N_h}(t))$ and introducing the *mass matrices* M and M^ε, the *stiffness matrices* K and B such that:

$$M_{k,j} = (\Phi_j,\Phi_k)\,, \quad M^\varepsilon_{k,j} = \left(\frac{\Phi_j}{|\nabla u|_\varepsilon},\Phi_k\right), \quad k,j = 1,\ldots,N_h$$

$$K_{k,j} = (\nabla\Phi_j,\nabla\Phi_k)\,, \qquad B_{k,j}(w) = \left(g(|\nabla w|^2)\frac{\nabla\Phi_j}{|\nabla u|_\varepsilon},\nabla\Phi_k\right)$$

the system on (4) can be written in matrix form as:

$$\begin{aligned}
M\underline{w}' + K\underline{w} = \gamma M(\underline{u} - \underline{w}), \quad \text{with } \underline{w}_0 = \underline{u}_0 \\
M_\varepsilon\underline{u}' + B(\underline{w})\underline{u} = K(\underline{u}_0 - \underline{u}), \quad \text{with } \underline{u}_0 = f_h
\end{aligned} \qquad (5)$$

where $f_h = \sum_{\ell=1}^{N_h} \alpha_\ell\Phi_\ell$ is the projection of the initial data on the space generated by the basis functions Φ_ℓ, $\ell = 1,\ldots,N_h$. The domain is discretized by a structure mesh whose vertices coincide with the image pixels. Both rectangular and triangular mesh elements can be used. The implementation of numerical methods for the solution of this coupled model is a difficult programming task. The problem stated in (5) is a system of nonlinear Ordinary Differential Equations which, depending on the parameter values, has a stiff behavior in the transient part of the solution (small time values) and the tends to converge to a smooth

equilibrium solution for large values of the time t. Therefore variable times steps and implicit or Backward Difference Methods are required. In order to evaluate the quality of the results on test images with different model parameters, we implemented the model equations using the Comsol Multiphysics environment (CM). The FEM solution is computed by means of the CM `femtime` function using linear lagrangian basis functions. CM provides an efficient ODE solver, the DASPK routine [15], which implements variable-order variable-stepsize backward differentiation formulas (BDF). Integrating the CM primitives with the Image Processing Toolbox of Matlab it is possible to build an application for testing the model (2) with different parameters and image noise types. A matlab script calling IPT and CM functions can be implemented with the following scheme:

- Image acquisition and noise perturbation (IPT);
- FEM solution (CM):
  - Mesh definition;
  - Model parameter setting;
  - Initial and boundary conditions setting;
  - Solution of the evolution problem (`femtime`);
- Results visualization and postprocessing (IPT).

CM provides a user friendly interactive interface for the setup of the FEM problem in the form given by (2). Once the solution is correctly defined it is possible to save it as an `.m` file that can be used as a matlab script changing the model parameter values for testing purpose.

4. Numerical Experiments

In this section we report the results obtained by smoothing and segmentation of some images using equations (2) applied to simulated and real dynamic MR data. The Gaussian and impulsive noise models are tested on different MR images obtaining good results in terms of noise removal and edge detection (see paragraphs 4.1 and 4.2).
In order to fairly compare the performance of the two models, we adopt the Improvement in Signal to Noise Ratio parameter (ISNR) [16]:

$$ISNR = 10log_{10}\left(\frac{\sum_{i,j}|f_{i,j} - g_{i,j}|^2}{\sum_{i,j}|f_{i,j} - \hat{f}_{i,j}|^2}\right)$$

where $f_{i,j}$, $g_{i,j}$ and $\hat{f}_{i,j}$ denote the original, degraded and filtered images, respectively. In general, the larger the $ISNR$ value, the better the performance.

The good performance of this model is also obtained in case of reduced encoding acquisition with noise in the Fourier data space (see paragraph 4.3).

4.1. **Gaussian Noise .** In the first experiment Gaussian white noise is added to the Brain image with SNR=10*db*. The original image is shown in figure (1(a)) and figure (1(b)) shows the noisy version of (a) obtained by adding gaussian white noise. Figures (2(a)) and (2(b)) respectively show the smoothed image u and the magnitude of $g(\nabla(w))$ obtained with model (2) at the higher ISNR value ($ISNR = 5.5$ at time $t = 22$). The parameter settings used to obtain these results where: $\beta = 0.01$, $K = 200$ and $k = \gamma = 0.1$.

(a) (b)

FIGURE 1. MR image (128×128): (a) original image; (b) Noisy Image: Gaussian additive white noise (SNR=10)

4.2. **Impulsive Noise.** In the second experiment we report the results obtained by the filter (2) in case of impulsive noise *salt and pepper*. The impulsive noise is added to the same image with $SNR = 10$ (see figure 3(a)). The edges of the noisy images are reported in figure 3(b) in terms of the magnitude of $g(\nabla(w))$. Figure (4) show the smoothed image u (figure 4(a)) and the magnitude of $g(\nabla(w))$ obtained at time $t = 3$ (figure 4(b)). The number of steps performed are 36 and the smallest integration step time used is 0.045.

The global behavior of the improvement parameter $ISNR$ over the entire integration interval shows the filtering performance of the model (2) with respect to the different noise models (figures 5(a) and 5(b)).

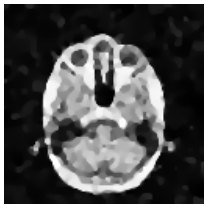

(a)

(b)

FIGURE 2. Smoothing and segmentation results of the noisy Mri image (128×128) using model (2); (a) Smoothed Image (t=22); (b) magnitude of $g(|\nabla(w)|)$

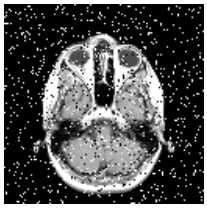

(a)

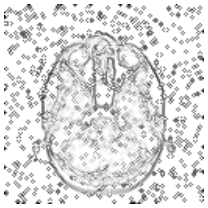

(b)

FIGURE 3. MR image (128×128): (a) Noisy Image: Salt and Pepper Noise (SNR=10); (b) magnitude of $g(|\nabla(w)|)$

4.3. **Dynamic MR experiment.** The dynamic MR test problem is constituted of a reference image (figure (6(a))) and a dynamic image (figure (6(b))) of 128×128 pixels. A set of $128 \times NL$ ($NL = 64$) data encodings are extracted from the dynamic image in the k-space and perturbed with additive gaussian white noise. Then the keyhole method is used to recover an approximation of the true dynamic image (figure (7(a))). In our test problem only the dynamic data are supposed to be affected by noise while the reference data are noiseless. In order to suppress the noisy artifacts of the Keyhole image the coupled diffusion filter is applied with $t \in [0, 3]$, using parameters values $k = 10$ and $\gamma = 10$; the smoothed image is shown in figure (7(b)). The noise

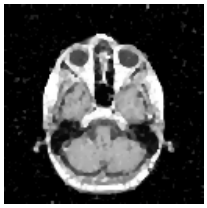

(a)

(b)

FIGURE 4. Smoothing and segmentation results of the noisy Mri image (128×128) using model (2); (a) Smoothed Image (t=3); (b) magnitude of $g(|\nabla(w)|)$

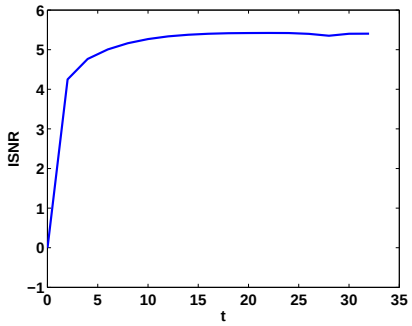

(a)

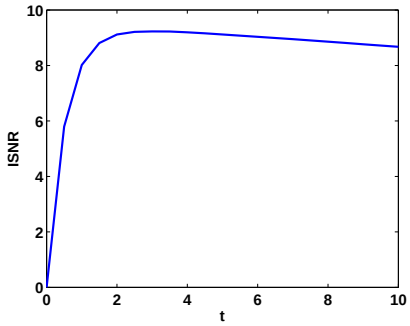

(b)

FIGURE 5. Parameter $ISNR$ over the entire integration interval: (a) $[0, 32]$ gaussian noise. (b) $[0, 10]$ Salt and Pepper noise.

reduction is particularly evident in terms of better edge detection as shown in figures(8(a)) and (8(b)).

The number of times steps required by the integration process is 25 and the smaller value of time interval is 0.0005. The size of the problem is 32768 degrees of freedom (DOF) the total computation time is 160 sec. on a 1.8Ghz Intel processor.

5. Conclusions

A matlab based application has been implemented to solve the denoising segmentation problem by means of a diffusion reaction coupled

(a) (b)

FIGURE 6. Functional Mri image (128×128): (a) Reference image; (b) Dynamic Image;

(a) (b)

FIGURE 7. (a) Keyhole reconstruction from 128×64 k-space samples with gaussian noise of variance 6. (b) Smoothed image at $t = 3$

PDE filter. The system is tested using Magnetic Resonance images affected by gaussian and impulsive noise obtaining an improvement of about $6db$. Furthermore functional magnetic resonance images are reconstructed from undersampled noisy data in the k-space, reporting good results in terms of artifacts removing and edges localization. A future development is the extension of this application to other more sophisticated coupled PDE filters.

REFERENCES

[1] L. I. Rudin, S. Osher, and E. Fatemi. Nonlinear total variation based noise removal algorithms. *Phys. D*, 60:259–268, 1992.

(a) (b)

FIGURE 8. Functional Mri image (128×128): (a) magnitude of $g(|\nabla(u)|)$ in the keyhole image; (b) magnitude of $g(|\nabla(u)|)$ in the smoothed.

[2] Z-P. Liang and P.C. Lauterbur. An efficient method for Dynamic Magnetic Resonance Imaging. *IEEE Trans. Med. Imag.*, 13(4):677–686, 1994.

[3] G. Landi, E. Loli Piccolomini, and F. Zama. A Total Variation-based regularization straegy in Magnetic Resonance Imaging. In R. P. Millane Editors P. J. Bones, M. A. Fiddy, editor, *Image Reconstruction from Incomplete Data III*, volume 5562 of *Proceedings of SPIE*, pages 141–151, 2004.

[4] G. Landi and E. Loli Piccolomini. A Total Variation regularization straegy in dynamic MRI. *Opt. Meth. Software*, 20(4-5):545–558, 2005.

[5] S. L. Keeling. Total Variation based convex filters for medical imaging. *Applied Math. and Comp.*, 139:101–119, 2003.

[6] P. Perona and J. Malik. Scale-Space and edge detection using anisotropic diffusion. *IEEE Trans. PAMI*, 12,(7), 629-639, 1990.

[7] F. Catte and P. L. Lions and J. M. Morel and T. Coll. Image selective smoothing and edge detection by nonlinear diffusion. *SIAM Journal of Numerical Analysis*, 29, 182-193, 1992.

[8] M. Nitzberg and T. Shiota. Nonlinear image filtering with edge corner enhancement. *IEEE trans. PAMI 14* (8), 826-832, 1992.

[9] L. Alvarez and P. L. Lions and J. M. Morel. Image selective smoothing and edge detection by nonlinear diffusion II. *SIAM Journal of Numerical Analysis*, 29 (3), 845-866, 1992.

[10] P. Charbonnier and L. Blanc-Feraud and G. Aubert and M. Barlaud. Two deterministic half-quadratic regularization algorithms for computed imaging. *In Proc. of IEEE Intl. Conf. on Image Processing (ICIP)*, (2), 168-173, 1994

[11] J. Li, *Finite element analysis and application for a onlinear diffusion model in image denoising*, Numer. Methods Partial Differential Eq. **18** (2002), 649–662.

[12] J. Weickert, *Anisotropic diffusion in image processing*, B.G. Teubner, 1998.

[13] Y. Chen, B.C. Vemuri, and Li Wang, *Image denoising and segmentation via nonlinear diffusion*, Comput. Math. Appl. **39** (2000), no. 5-6, 131–149.

[14] D. Barash, T. Schlick, M. Israeli, and R. Kimmel, *Multiplicative operator splittings in nonlinear diffusion: From spatial splitting to multiple timesteps*, J. of Mathematical Imaging and Vision **19** (2003), 33–48.
[15] P. N. Brown, A. C. Hindmarsh, and L. R. Petzold, *Using krylov methods in the solution of large-scale differential-algebraic systems*, SIAM J. Sci. Comput. **15** (1994), 1467–1488.
[16] M.R. Banham and A.K. Katsaggelos, *Digital image restoration*, IEEE Signal Process. Mag. **14** (1997), no. 2, 2441.
[17] V. Thomee, *Galerkin finite element methods for parabolic problems*, Springer Series in Computational Mathematics, vol. 25, Springer, 1997.
[18] G. Landi, E. Loli Piccolomini, and F. Zama. A total variation-based reconstruction method for dynamic mri. *COMPUTATIONAL AND MATHEMATICAL METHODS IN MEDICINE*, 175:715–729, 2008. (ISSN:1748-670X).

Department of Mathematics, Piazza Porta S. Donato 5, 40126 Bologna